Theor Chim Acta (1995) 90: 441–458

Theoretica Chimica Acta

Ab initio calculation of electronic circular dichroism for *trans*-cyclooctene using London atomic orbitals*

Keld L. Bak[1], Aage E. Hansen[1], Kenneth Ruud[2], Trygve Helgaker[2], Jeppe Olsen[3], Poul Jørgensen[4]

[1] Department of Physical Chemistry, Copenhagen University, DK-2100 Copenhagen Ø, Denmark

[2] Department of Chemistry, University of Oslo, Blindern, N-0315 Oslo, Norway

[3] Theoretical Chemistry, Chemical Centre, University of Lund, P.O. Box 124, S-22100 Lund, Sweden

[4] Department of Chemistry, Aarhus University, DK-8000 Aarhus C, Denmark

Received May 31, 1994/Final revision received August 16, 1994/Accepted September 26, 1994

Summary. The second-quantization magnetic dipole operator that arises when London atomic orbitals are used as basis functions is derived. In atomic units, the magnetic dipole operator is defined as the negative of the first derivative of the electronic Hamiltonian containing the interaction with the external magnetic field. It is shown that for finite basis sets, the gauge origin dependence of the resulting magnetic dipole operator is analogous to that of the exact operator, and that the derived operator converges to the exact operator in the limit of a complete basis set. It is also demonstrated that the length expression for the rotatory strength in linear response calculations gives gauge-origin-independent results. Sample calculations on *trans*-cyclooctene and its fragments are presented. Compared to conventional orbitals, the basis set convergence of the rotatory strengths calculated in the length form using London atomic orbitals is favourable. The rotatory strength calculated for *trans*-cyclooctene agrees nicely with the corresponding experimental circular dichroism spectrum, but the spectra for the fragment molecules show little resemblance with that of *trans*-cyclooctene.

Key words: Electronic circular dichroism – *Trans*-cyclooctene – London atomic orbitals

1. Introduction

The differential absorption in the visible and ultraviolet regions of optically active molecules is referred to as electronic circular dichroism (ECD) or just circular dichroism (CD) and is determined by the electronic rotatory strength [1]. The sign of the rotatory strength is characteristic for the individual isomers of a pair of enantiomers. The rotatory strength corresponds to the imaginary part of the dot product of the electric and magnetic transition dipole moments [1]. In finite basis calculations, the length expression of the rotatory strength is gauge-origin dependent, whereas the velocity expression is gauge-origin independent [1]. Finite basis set calculations of the dipole length transition moments converge faster toward basis set limit results than the corresponding dipole velocity calculations. From

* Dedicated to Prof. Jan Linderberg

a computational point of view the length expression is therefore to be preferred, whereas from a gauge-origin point of view the velocity representation must be preferred. In this paper we show that when the perturbation-dependent London atomic orbitals (LAO) are used [2], the length expression of the rotatory strength becomes gauge-origin independent.

London atomic orbitals, which by some authors are referred to as gauge invariant or gauge including atomic orbitals (GIAO), have previously been used successfully in calculations of a variety of magnetic molecular properties [2–15]. These include the pioneering calculations of nuclear magnetic shieldings and magnetizabilities by London [2], Hameka [3, 4], and McWeeny [5], the calculations of magnetic circular dichroism by Seamans and Linderberg [6], and the calculations of g-tensors for electron spin resonance by Dalgaard [7]. Later *ab initio* calculations include nuclear shieldings [8–11], magnetizabilities [12, 13], and the atomic axial tensors entering the intensity expression for vibrational circular dichroism [14, 15]. Besides giving gauge-origin-independent magnetic properties, LAO calculations have been shown to have superior basis set convergence characteristics compared to approaches where perturbation-dependent basis set are not used. This faster convergence arises since for a one-electron system the LAOs respond correctly to a magnetic field through first order. In this paper we compare the basis convergence of rotatory strengths calculated in the random phase approximation [16, 17] (RPA) from the length and velocity expressions using ordinary basis set and from the length expression using LAO's.

The rotatory strength corresponds to the residue of the electric dipole–magnetic dipole linear response function [17, 18]. In a companion paper we show how linear response functions and their residues can be obtained from perturbation-dependent basis sets [19]. In this paper, we consider the calculation of rotatory strengths using the perturbation-dependent LAOs. The LAO magnetic dipole operator is defined as the negative of the first derivative of the second-quantization electronic Hamiltonian in the limit of zero magnetic field. The second-quantization Hamiltonian contains interaction terms due to the external magnetic field. In addition, the basis set dependence of the magnetic field is incorporated in this Hamiltonian. We prove that in the limit of a complete basis set, this magnetic dipole operator becomes identical to the conventional dipole operator. As shown in the companion paper [19], it is convenient to use the so-called *natural orbital connection* for deriving this first derivative Hamiltonian. If this connection is used, the conventional magnetic dipole operator is obtained in the limit of a complete basis even if the terms coming from the differentiated creation and annihilation operators are neglected. This is not true for any other connection. We refer to the companion paper for a more detailed discussion of this point [19].

We have implemented the theory for London ECD in a computer program, and sample RPA calculations of the rotatory strength for *trans*-cyclooctene are reported. The experimental CD and absorption spectra for this molecule are known [20], and semiempirical [21] as well as *ab initio* calculations using conventional basis sets have been reported [22]. See Ref. [22] for a survey of earlier calculations and interpretations.

The theoretical implications of using LAOs in calculations of magnetic dipole moments and electronic rotatory strengths are discussed in the next section. In particular, the magnetic dipole operator as defined above is derived and analyzed separately and in conjunction with ECD calculations. In Section 3 we report calculations on *trans*-cyclooctene and its fragments. The basis set convergence of the rotatory strength is compared for calculations performed with LAOs and with

ordinary atomic orbitals. The absorption and CD spectra of *trans*-cyclooctene (based on the eight lowest excitations of A and B symmetries) are computed and compared with the experiment and with spectra calculated for the fragment molecules. The last section contains some concluding remarks.

2. Theory

The differential intensities observed in circular dichroism spectra are determined by the rotatory strength, which for a transition between Ψ_0 and Ψ_n corresponds to the imaginary part of the dot product between the electric and magnetic transition dipole moments [1]

$$R(0 \to n) = \mathrm{Im}[\langle \Psi_0 | \boldsymbol{\mu}_{\mathrm{el}} | \Psi_n \rangle \langle \Psi_n | \boldsymbol{\mu}_{\mathrm{mag}} | \Psi_0 \rangle]. \tag{1}$$

The electronic and magnetic dipole operators $\boldsymbol{\mu}_{\mathrm{el}}$ and $\boldsymbol{\mu}_{\mathrm{mag}}$ are in atomic units given by the expressions

$$\boldsymbol{\mu}_{\mathrm{el}} = -\sum_i \boldsymbol{r}_i + \sum_M Z_M \boldsymbol{R}_M, \tag{2}$$

$$\boldsymbol{\mu}_{\mathrm{mag}} = -\frac{1}{2}\sum_i \boldsymbol{r}_i \times \boldsymbol{p}_i + \sum_M \left(\frac{Z_M}{2M_M}\right) \boldsymbol{R}_M \times \boldsymbol{P}_M, \tag{3}$$

where $\boldsymbol{r}_i$ and $\boldsymbol{p}_i$ are the position and momentum of the ith electron, and Z_M, M_M, $\boldsymbol{R}_M$, and $\boldsymbol{P}_M$ are the charge, mass, position, and momentum of the Mth nucleus. The expressions (1)–(3) correspond to the so-called length formulation of the rotatory strength.

CD as observed in visible and ultraviolet spectroscopy is assigned to electronic transitions and termed electronic circular dichroism (ECD). *Ab initio* calculations of ECD and electronic absorptions are in the Born–Oppenheimer approximation carried out for a particular molecular conformation. In this approximation, Ψ_0 and Ψ_n in Eq. (1) are electronic wave functions, and the terms involving the nuclear parts of the electric and magnetic dipole transition elements therefore vanish. Changing the gauge origin from $\boldsymbol{O}$ to $\boldsymbol{O}_1 = \boldsymbol{O} + \boldsymbol{V}$ leaves $\boldsymbol{p}_i$ invariant but changes $\boldsymbol{r}_i$ to $\boldsymbol{r}_i - \boldsymbol{V}$. While the electric transition dipole moment is unaltered by such a shift of origin, the magnetic transition dipole moment changes:

$$-\frac{1}{2}\left\langle \Psi_0 \left| \sum_i (\boldsymbol{r}_i - \boldsymbol{V}) \times \boldsymbol{p}_i \right| \Psi_n \right\rangle = -\frac{1}{2}\left\langle \Psi_0 \left| \sum_i \boldsymbol{r}_i \times \boldsymbol{p}_i \right| \Psi_n \right\rangle + \frac{1}{2}\boldsymbol{V} \times \left\langle \Psi_0 \left| \sum_i \boldsymbol{p}_i \right| \Psi_n \right\rangle. \tag{4}$$

As is seen from the hypervirial theorem, for exact wave functions, $\langle \Psi_0 | \sum_i \boldsymbol{p}_i | \Psi_n \rangle$ is parallel to $\langle \Psi_0 | \sum_i \boldsymbol{r}_i | \Psi_n \rangle$ and the length form of the rotatory strength is then origin independent, while for finite basis sets this is in general not true. One remedy is to use the dipole velocity approximation for the electric dipole transition elements, since the rotatory strength is then origin independent also for approximate wave functions. Another solution is to use London orbitals, for which we will show that the length expression in Eq. (1) also becomes gauge-origin independent.

A. The effective angular momentum operator for finite basis sets using London atomic orbitals

In first quantization, the angular momentum operator is obtained by differentiating the electronic Hamiltonian that contains the magnetic interaction once with respect to the external magnetic field, multiplying by a factor of two, and taking the zero-field limit. In analogy, we define the second-quantization angular momentum operator as the zero-field limit of the second-quantization electronic Hamiltonian differentiated with respect to the field and multiplied by two. In atomic units, the magnetic dipole operator for a singlet state is obtained by multiplying the angular momentum operator by $-\frac{1}{2}$. Since the operators of second quantization are projected onto the space spanned by the basis functions, they depend on this basis. Therefore, the use of LAOs will be reflected in the actual form of the magnetic dipole operator.

The derivation builds extensively on the following three papers: The first, by Helgaker and Jørgensen [23], is referred to as Paper 1, the second, by Bak et al. [14], is referred to as Paper 2, and the third, by Olsen et al. [19], is referred to as Paper 3.

In Paper 1 the second-quantization electronic Hamiltonian appropriate for magnetic property calculations with LAOs is expanded in the magnetic field. From our previous definition it may sound as if the magnetic dipole operator was basically obtained in Paper 1. However, this is not the case. The expansion of the Hamiltonian in Paper 1 was intended only for calculations of differentiated expectation values. The terms emerging from differentiated creation and annihilation operators were therefore ignored. In order to obtain the magnetic dipole operator, these terms must also be considered.

Paper 2 concerns vibrational circular dichroism and includes both the general formula for differentiated creation operators and the specific formula for differentiation with respect to magnetic field when LAOs are used.

The second-quantization magnetic dipole operator can be obtained from Papers 1 and 2, but in these papers the orthogonal molecular orbitals were connected from one value of $\boldsymbol{B}$ to another by the *symmetric connection*. In this work we use the *natural connection* introduced in Paper 3. This connection ensures that orthogonal molecular orbitals at different $\boldsymbol{B}$ values are as similar as possible to the field free orbitals. The natural connection results in an easier and more elegant derivation of the angular momentum operator. To demonstrate this point, we here also derive the operator using the symmetric connection.

As discussed in Paper 1, the second-quantization spin-free non-relativistic electronic Hamiltonian for a system exposed to a magnetic field represented by the vector potential $\boldsymbol{A}$ is

$$\hat{H}(\boldsymbol{A}) = \sum_{mn} \tilde{h}_{mn}(\boldsymbol{A}) E_{mn}(\boldsymbol{A}) + \frac{1}{2} \sum_{mnpq} \tilde{g}_{mnpq}(\boldsymbol{A}) e_{mnpq}(\boldsymbol{A}). \tag{5}$$

Since we consider a situation where the magnetic moments are all zero, the magnetic vector potential as function of the position $\boldsymbol{v}$ is

$$\boldsymbol{A}(\boldsymbol{v}) = \tfrac{1}{2}\boldsymbol{B} \times (\boldsymbol{v} - \boldsymbol{O}), \tag{6}$$

where $\boldsymbol{B}$ is the magnetic field and $\boldsymbol{O}$ the gauge origin. The integrals $\tilde{h}_{mn}(\boldsymbol{A})$ and $\tilde{g}_{mnpq}(\boldsymbol{A})$ as well as the excitation operators $E_{mn}(\boldsymbol{A})$ and $e_{mnpq}(\boldsymbol{A})$ refer to a set of

orthonormal molecular orbitals (OMOs) expanded in LAOs. The LAOs are defined as [2]

$$\omega_\mu(\boldsymbol{A}_\mu^c) = \exp(-\mathrm{i}\boldsymbol{A}_\mu^c \cdot \boldsymbol{r})\chi_\mu, \tag{7}$$

where $\chi_\mu = \chi_\mu(\boldsymbol{r} - \boldsymbol{R}_\mu)$ is an atomic orbital (AO) centred on a nucleus at $\boldsymbol{R}_\mu$, $\boldsymbol{r}$ denotes electron coordinates, and

$$\boldsymbol{A}_\mu^c = \tfrac{1}{2}\boldsymbol{B} \times (\boldsymbol{R}_\mu - \boldsymbol{O}) \tag{8}$$

is the magnetic vector potential found at the position $\boldsymbol{R}_\mu$. The so-called unmodified molecular orbitals (UMOs) are defined as linear combinations of the LAOs:

$$\psi_i(\boldsymbol{A}^c) = \sum_\mu K_{\mu i}(\boldsymbol{B}_0)\omega_\mu(\boldsymbol{A}_\mu^c). \tag{9}$$

The expansion coefficients $K_{\mu i}(\boldsymbol{B}_0)$ are the amplitudes for the optimized molecular orbitals at the reference field $\boldsymbol{B}_0$, which in this work is equal to zero. In general, the UMOs are non-orthogonal. The set of OMOs is expanded in the set of UMOs as

$$\varphi_i(\boldsymbol{A}^c) = \sum_j T_{ji}(\boldsymbol{A}^c)\psi_j(\boldsymbol{A}^c), \tag{10}$$

where the expansion coefficients $T_{ji}(\boldsymbol{A}^c)$ depend on $\boldsymbol{A}^c$. The orthonormality requirements on the OMOs for all $\boldsymbol{B}$ together with additional conditions needed to specify $\boldsymbol{T}$ uniquely, define the various orbital connection schemes. As already noted we will consider the natural and symmetric connections, but for now the connection is unspecified.

Using our definition of the second-quantization angular momentum operator (twice the zero-field value of the first derivative of the electronic Hamiltonian with respect to $\boldsymbol{B}$ for zero nuclear magnetic moments), we obtain from Eq. (5) the magnetic dipole operator

$$\hat{L}(\boldsymbol{O}) = 2\Bigg[\sum_{mn}(\tilde{h}_{mn}^{(\boldsymbol{B})}(\boldsymbol{O})E_{mn} + \tilde{h}_{mn}E_{mn}^{(\boldsymbol{B})}(\boldsymbol{O})) + \frac{1}{2}\sum_{mnpq}(\tilde{g}_{mnpq}^{(\boldsymbol{B})}(\boldsymbol{O})e_{mnpq} + \tilde{g}_{mnpq}e_{mnpq}^{(\boldsymbol{B})}(\boldsymbol{O}))\Bigg]. \tag{11}$$

The superscripts $(\boldsymbol{B})$ indicate first-order differentiation with respect to $\boldsymbol{B}$.

To bring the angular momentum operator into a more useful form, we must evaluate the terms on the right-hand side. Using Eq. (10), it is straightforward to re-express the OMOs in Eq. (11) in terms of integrals over UMOs, taking advantage of the fact that Eq. (11) represents the zero-field limit:

$$\tilde{h}_{mn} = h_{mn}, \tag{12}$$

$$\tilde{h}_{mn}^{(\boldsymbol{B})} = h_{mn}^{(\boldsymbol{B})} + \sum_o (T_{mo}^{(\boldsymbol{B})}h_{on} + T_{no}^{(\boldsymbol{B})*}h_{mo}), \tag{13}$$

$$\tilde{g}_{mnpq} = g_{mnpq}, \tag{14}$$

$$\tilde{g}_{mnpq}^{(\boldsymbol{B})} = g_{mnpq}^{(\boldsymbol{B})} + \sum_o (T_{mo}^{(\boldsymbol{B})}g_{onpq} + T_{no}^{(\boldsymbol{B})*}g_{mopq} + T_{po}^{(\boldsymbol{B})}g_{mnoq} + T_{qo}^{(\boldsymbol{B})*}g_{mnpo}). \tag{15}$$

Using Eq. (9), all the UMO integrals except the differentiated connection matrix can be rewritten in terms of AO integrals

$$h_{mn} = \sum_{\mu\nu} K^*_{\mu m} K_{\nu n} h_{\mu\nu}, \tag{16}$$

$$h^{(B)}_{mn} = \sum_{\mu\nu} K^*_{\mu m} K_{\nu n} h^{(B)}_{\mu\nu}, \tag{17}$$

$$g_{mnpq} = \sum_{\mu\nu\rho\sigma} K^*_{\mu m} K_{\nu n} K^*_{\rho p} K_{q\sigma} g_{\mu\nu\rho\sigma}, \tag{18}$$

$$g^{(B)}_{mnpq} = \sum_{\mu\nu\rho\sigma} K^*_{\mu m} K_{\nu n} K^*_{\rho p} K_{q\sigma} g^{(B)}_{\mu\nu\rho\sigma}, \tag{19}$$

In order to express the differentiated connection matrix as linear combinations of atomic integrals, we must specify the connection. According to Paper 3, in the natural connection the differentiated connection matrix becomes

$$T^{(B)}_{mn} = -\sum_{\mu\nu} K^*_{\mu m} K_{\nu n} \left\langle \chi_\mu \middle| \frac{\partial \omega_\nu}{\partial \boldsymbol{B}} \right\rangle. \tag{20a}$$

Alternatively, if the symmetric connection is used we know from Papers 1 and 2 that the differentiated connection takes the form

$$T^{(B)}_{mn} = -\frac{1}{2} \sum_{\mu\nu} K^*_{\mu m} K_{\nu n} \frac{\partial}{\partial \boldsymbol{B}} \langle \omega_\mu | \omega_\nu \rangle. \tag{20b}$$

Denoting the first-quantization one-electron part of the electronic Hamiltonian by h, and the distance from electron 1 to electron 2 by r_{12}, the AO integrals on the right-hand side of the Eqs. (16)–(20b) are

$$h_{\mu\nu} = \langle \chi_\mu(\boldsymbol{r}) | h | \chi_\nu(\boldsymbol{r}) \rangle, \tag{21}$$

$$h^{(B)}_{\mu\nu} = \tfrac{1}{2} \langle \chi_\mu(\boldsymbol{r}) | -\mathrm{i}(\boldsymbol{r} - \boldsymbol{R}_\nu) \times \nabla + (\boldsymbol{X}_\mu - \boldsymbol{X}_\nu) h | \chi_\nu(\boldsymbol{r}) \rangle, \tag{22}$$

$$g_{\mu\nu\rho\sigma} = \frac{1}{2} \left\langle \chi_\mu(\boldsymbol{r}_1) \chi_\rho(\boldsymbol{r}_2) \middle| \frac{1}{r_{12}} \middle| \chi_\nu(\boldsymbol{r}_1) \chi_\sigma(\boldsymbol{r}_2) \right\rangle, \tag{23}$$

$$g^{(B)}_{\mu\nu\rho\sigma} = \frac{1}{2} \left\langle \chi_\mu(\boldsymbol{r}_1) \chi_\rho(\boldsymbol{r}_2) \middle| \frac{\boldsymbol{X}_\mu(\boldsymbol{r}_1) - \boldsymbol{X}_\nu(\boldsymbol{r}_1) + \boldsymbol{X}_\rho(\boldsymbol{r}_2) - \boldsymbol{X}_\sigma(\boldsymbol{r}_2)}{r_{12}} \middle| \chi_\nu(\boldsymbol{r}_1) \chi_\sigma(\boldsymbol{r}_2) \right\rangle, \tag{24}$$

$$\left\langle \chi_\mu \middle| \frac{\partial \omega_\nu}{\partial \boldsymbol{B}} \right\rangle = -\tfrac{1}{4} \langle \chi_\mu(\boldsymbol{r}) | 2\boldsymbol{X}_\nu - \boldsymbol{Y}(\boldsymbol{O}) | \chi_\nu(\boldsymbol{r}) \rangle, \tag{25}$$

$$\frac{\partial}{\partial \boldsymbol{B}} \langle \omega_\mu | \omega_\nu \rangle = \tfrac{1}{2} \langle \chi_\mu(\boldsymbol{r}) | \boldsymbol{X}_\nu - \boldsymbol{X}_\nu | \chi_\nu(\boldsymbol{r}) \rangle. \tag{26}$$

We have here used the shorthand notation

$$\boldsymbol{X}_\mu = \boldsymbol{X}_\mu(\boldsymbol{r}) \equiv \mathrm{i}\boldsymbol{R}_\mu \times \boldsymbol{r} \tag{27}$$

$$\boldsymbol{Y}(\boldsymbol{O}) = \boldsymbol{Y}(\boldsymbol{r}, \boldsymbol{O}) \equiv \mathrm{i}2\boldsymbol{O} \times \boldsymbol{r} \tag{28}$$

To specify the angular momentum operator completely, we must also detail the differentiated excitation operators. The excitation operators are defined in terms of the creation and the annihilation operators $a^+_{m\sigma}(\boldsymbol{A}^e)$ and $a_{n\sigma}(\boldsymbol{A}^e)$, which create and

annihilate electrons in the OMOs and therefore in the LAO representation depend on A^c rather than A. The excitation operators are

$$E_{mn}(A^c) = \sum_\sigma a^+_{m\sigma}(A^c)a_{n\sigma}(A^c), \tag{29}$$

$$e_{mnpq}(A^c) = E_{mn}(A^c)E_{pq}(A^c) + \delta_{pn}E_{mq}(A^c), \tag{30}$$

where the summation in Eq. (29) is over spin. It is shown in Paper 2 that the differentiated excitation operators become

$$E^{(B)}_{mn}(O) = \sum_r (D^{(B)}_{rm}(O)E_{rn} + D^{(B)*}_{rn}(O)E_{mr}) + E^{(B)}_{\perp mn}(O), \tag{31}$$

$$e^{(B)}_{mnpq}(O) = E^{(B)}_{mn}(O)E_{pq} + E_{mn}E^{(B)}_{pq}(O) + \delta_{pn}E^{(B)}_{mq}(O), \tag{32}$$

with

$$E^{(B)}_{\perp mn}(O) \equiv \sum_\sigma (a^{(B)+}_{m\sigma\perp}(O)a_{n\sigma} + a^+_{m\sigma}a^{(B)}_{n\sigma\perp}(O)). \tag{33}$$

Here $a^{(B)+}_{\perp m\sigma}(O)$ and $a^{(B)}_{\perp n\sigma}(O)$ are the parts of $\partial a^+_{m\sigma}(A^c)/\partial B$ and $\partial a_{n\sigma}(A^c)/\partial B$ at zero field that cannot be expanded in the original set of creation and annihilation operators. The expansion coefficients $D^{(B)}_{mn}(O)$ are the elements of an anti-Hermitian matrix, whose explicit form depends on the connection. According to Paper 3, these coefficients vanish for the natural connection:

$$D^{(B)}_{mn}(O) = 0. \tag{34a}$$

If instead the symmetric connection is used, we have shown in Paper 2 that the matrix has the form

$$D^{(B)}_{mn}(O) = -\frac{1}{4}\sum_{\mu\nu} K^*_{\mu m}K_{\nu n}\langle\chi_\mu(r)|X_\mu + X_\nu - Y(O)|\chi_\nu(r)\rangle. \tag{34b}$$

The final expression for the angular momentum operator can now be obtained by inserting Eqs. (12)–(34b) into Eq. (11) and by using the commutator relation

$$[X_\mu, h] = iR_\mu \times \nabla. \tag{35}$$

At this point we must choose connection. For the natural connection, Eqs. (20a) and (34a) should be used and for the symmetric connection we use Eqs. (20b) and (34b). In either case, the resulting angular momentum operator is

$$\begin{aligned}\hat{L}(O) = \sum_{mn}\Bigg\{&\sum_{\mu\nu} K^*_{\mu m}K_{\nu n}\langle\mu|\,-ir\times\nabla + X_\mu h - hX_\nu|\nu\rangle \\ &+\frac{1}{2}\sum_r\sum_{\mu\nu}(K^*_{\mu r}K_{\nu n}h_{mr}\langle\mu|2X_\nu - Y(O)|\nu\rangle \\ &- K^*_{\mu m}K_{\nu r}\langle\mu|2X_\mu - Y(O)|\nu\rangle h_{rn})\Bigg\}E_{mn} \\ &+\sum_{mnpq}\Bigg\{\sum_{\mu\nu\rho\sigma} K^*_{\mu m}K_{\nu n}K^*_{\rho p}K_{\sigma q} \\ &\times\left\langle\mu(r_1)\rho(r_2)\left|\frac{X_\mu(r_1) - X_\nu(r_1) + X_\rho(r_2) - X_\sigma(r_2)}{r_{12}}\right|\nu(r_1)\sigma(r_2)\right\rangle\end{aligned}$$

$$-\frac{1}{4}\sum_{r}\sum_{\mu\nu}[K^{*}_{\mu m}g_{rnpq}+K^{*}_{\mu p}g_{mnrq})K_{\nu r}\langle\mu|2\boldsymbol{X}_{\mu}-\boldsymbol{Y}(\boldsymbol{O})|\nu\rangle$$

$$-(K_{\nu n}g_{mrpq}+K_{\nu q}g_{mnpr})K^{*}_{\mu r}\langle\mu|2\boldsymbol{X}_{\nu}-\boldsymbol{Y}(\boldsymbol{O})|\nu\rangle]\Big\}e_{mnpq}$$

$$+2\sum_{mn}h_{mn}E^{(B)}_{\perp mn}(\boldsymbol{O})+\sum_{mnpq}g_{mnpq}(E^{(B)}_{\perp mn}(\boldsymbol{O})E_{pq}+E_{mn}E^{(B)}_{\perp pq}(\boldsymbol{O})$$

$$+\delta_{pn}\mathrm{E}^{(B)}_{\perp mq}(\boldsymbol{O})\delta_{pn}). \tag{36}$$

Although the form of this operator is strongly influenced by the use of London orbitals, the integrals are all standard AOs. It is interesting to notice that the angular momentum operator is a two-electron operator, somewhat surprising since the first-quantization angular momentum operator is a one-electron operator. However, in the limit of a complete basis the operator in Eq. (36) becomes identical to the projected first-quantization operator as demonstrated in Paper 3. We give an alternative proof in Sect. 2B. In Sect. 2C we demonstrate that the gauge-origin dependence of the angular momentum operator in Eq. (36) corresponds exactly to the gauge dependence of the exact operator, even for finite basis sets. This result holds only for the complete operator in Eq. (36). Using the magnetic dipole operator obtained from the angular momentum operator together with the conventional electric dipole operator, we also show that rotatory strengths in RPA and multi-configurational (MC) RPA [24] are gauge-origin independent for finite basis sets.

Before proceeding with these proofs, we comment on some of the characteristics of the natural and the symmetric connections. In the natural connection, the differentiated creation operators only contribute with terms from the orthogonal complement of the basis set. Therefore, all contributions to the angular momentum operator that can be expanded in our basis arise only through differentiation of the matrix elements. Moreover, these are the only contributions to expectation and transition values.

When the symmetric connection is used, differentiated creation operators contribute with terms that are both inside and outside the basis set. In the symmetric connection the contributions from the differentiated matrix elements are independent of the gauge origin. The exact operator is gauge dependent, and in the symmetric connection this dependence arises through the differentiation of the creation and annihilation operators. The operator obtained by differentiating only matrix elements is unphysical in the symmetric connection.

B. The angular momentum operator in the limit of a complete basis set

The first thing to notice when discussing the LAO angular momentum operator (36) in a complete basis set, is that the terms involving $E^{(B)}_{\perp mn}(\boldsymbol{O})$ vanish since there is no orthogonal complement to the basis. In the limit of a complete basis set we can also use the identity

$$\sum_{r}|r\rangle\langle r|=1 \tag{37}$$

to show that

$$\sum_r \sum_{\mu\nu} K^*_{\mu m} K_{\nu r} g_{rnpq} \langle \mu | 2X_\mu - Y(O) | \nu \rangle$$

$$= \sum_{\mu\nu\rho\sigma} K^*_{\mu m} K_{\nu n} K^*_{\rho p} K_{\sigma q} \left\langle \mu(r_1)\rho(r_2) \left| \frac{2X_\mu(r_1) - Y(r_1, O)}{r_{12}} \right| \nu(r_1)\sigma(r_2) \right\rangle \tag{38}$$

and the two-electron terms in the angular momentum operator therefore disappear. Using the commutator relation

$$[Y(O), h] = \mathrm{i}2O \times \nabla, \tag{39}$$

and the resolution of identity, Eq. (37), we obtain for the remaining one-electron terms of the LAO angular momentum operator

$$\hat{L}(O) = \sum_{mn} \langle m | L(O) | n \rangle E_{mn}. \tag{40}$$

The first-quantization angular momentum operator appearing on the right-hand side is

$$L(O) \equiv -i(r - O) \times \nabla. \tag{41}$$

Therefore, for complete basis sets the LAO magnetic dipole operator reduces to a one-electron operator that is identical to the usual second-quantization angular momentum operator.

C. Gauge origin dependence of the angular momentum operator and of the rotatory strength

When the angular momentum operator in Eq. (36) is used to compute expectation values and transition matrix elements, all terms containing $E^{(B)}_{\perp mn}(O)$ vanish. To simplify our discussion we neglect these terms in the following and we do so without specifically denoting this in the notation.

Consider changing the gauge origin from O to O_1:

$$O_1 = O + V. \tag{42}$$

The LAO angular momentum operator for the new gauge origin becomes

$$\hat{L}(O_1) = \hat{L}(O) + \mathrm{i}V \times \sum_{mn} \sum_r (\langle m | r | r \rangle h_{rn} - h_{mr} \langle r | r | n \rangle) E_{mn}$$

$$+ \frac{\mathrm{i}}{2} V \times \sum_{mnpq} \sum_r (\langle m | r | r \rangle g_{rnpq} - g_{mrpq} \langle r | r | n \rangle$$

$$+ \langle p | r | r \rangle g_{mnrq} - g_{mnpr} \langle r | r | q \rangle) e_{mnpq}. \tag{43}$$

Using the commutator relations

$$[E_{mn}, E_{pq}] = \delta_{pn} E_{mq} - \delta_{mq} E_{pn}, \tag{44}$$

$$[E_{rs}, e_{mnpq}] = \delta_{ms} e_{rnpq} - \delta_{rn} e_{mspq} + \delta_{ps} e_{mnrq} - \delta_{rq} e_{mnps}, \tag{45}$$

which hold for finite as well as complete basis sets, Eq. (43) can be rewritten as

$$\hat{L}(O_1) = \hat{L}(O) + \mathrm{i}V \times [\hat{r}, \hat{H}], \tag{46}$$

where we have defined

$$\hat{\boldsymbol{r}} = \sum_{mn} \langle m|\boldsymbol{r}|n\rangle E_{mn}. \tag{47}$$

In RPA [16, 17] and MC-RPA [24], the equations of motion for the linear response function ensure that

$$\langle \Psi_0|[\hat{\boldsymbol{r}}, \hat{H}]|\Psi_n\rangle = \omega_n \langle \Psi_0|\hat{\boldsymbol{r}}|\Psi_n\rangle, \tag{48}$$

where ω_n is the excitation energy for the transition $\Psi_0 \rightarrow \Psi_n$. Therefore, the transition matrix element of $i\boldsymbol{V}\times[\hat{\boldsymbol{r}}, \hat{H}]$ is orthogonal to the corresponding transition matrix elements of the electric dipole operator

$$\boldsymbol{\mu}_{\mathrm{el}} = -\hat{\boldsymbol{r}}. \tag{49}$$

Hence, with the magnetic dipole operator defined from the LAO angular momentum operator in Eq. (36) as

$$\boldsymbol{\mu}_{\mathrm{mag}}(\boldsymbol{O}) = -\tfrac{1}{2}\hat{\boldsymbol{L}}(\boldsymbol{O}), \tag{50}$$

the rotatory strength obtained from Eq. (1) using RPA and MC-RPA is gauge-origin independent for finite basis sets. In complete basis sets the left-hand-side of Eq. (48) is proportional to $\langle \Psi_0|\hat{\nabla}|\Psi_n\rangle$ by the RPA and MC-RPA hypervirial relation, and the LAO rotatory strength in the velocity form is also gauge-origin invariant in this limit. By the same token the LAO velocity rotatory strength is not gauge-origin invariant for finite basis sets, in contrast to the situation for conventional basis sets.

D. Magnetic transition dipole moment from linear response theory

The magnetic transition dipole moment and the rotatory strength may be calculated from the residues of the linear response functions. To see this, we consider the time development of the average value of $\hat{\boldsymbol{\mu}}_{\mathrm{mag}}$ for a state $|O\rangle$ which responds to a time-dependent electric field resulting in the perturbation

$$\hat{V}^t = \int_{-\infty}^{\infty} \mathrm{d}\omega_1 \, \hat{\boldsymbol{\mu}}_{\mathrm{el}} \exp[(-i\omega_1 + \varepsilon)t]. \tag{51}$$

Here ω_1 is the frequency of the field and ε a positive infinitesimal. Using overbar for the time-dependent perturbed state and no bar for the time-independent unperturbed state, the average value can be expanded in orders of the perturbations [18]

$$\langle \bar{\mathrm{O}}|\hat{\boldsymbol{\mu}}_{\mathrm{mag}}|\bar{\mathrm{O}}\rangle = \langle \mathrm{O}|\hat{\boldsymbol{\mu}}_{\mathrm{mag}}|\mathrm{O}\rangle + \int_{-\infty}^{\infty} \mathrm{d}\omega_1 \exp[(-i\omega_1 + \varepsilon)t] \times \langle\langle \hat{\boldsymbol{\mu}}_{\mathrm{mag}}; \hat{\boldsymbol{\mu}}_{\mathrm{el}}\rangle\rangle_{\omega_1 + i\varepsilon} + \cdots \tag{52}$$

and the residues of the linear response function are given by [18]

$$\lim_{\omega_1 \rightarrow \omega_n} (\omega_1 - \omega_n)\langle\langle \hat{\boldsymbol{\mu}}_{\mathrm{mag}}; \hat{\boldsymbol{\mu}}_{\mathrm{el}}\rangle\rangle_{\omega_1} = \langle \mathrm{O}|\hat{\boldsymbol{\mu}}_{\mathrm{mag}}|n\rangle\langle n|\hat{\boldsymbol{\mu}}_{\mathrm{el}}|\mathrm{O}\rangle. \tag{53}$$

Hence, the magnetic transition dipole moment and the rotatory strengths can be evaluated from the residue. From Eq. (52) it is also seen that the last two terms in Eq. (36), which describe the part of the field dependence of the creation and annihilation operators that cannot be expanded in the unperturbed orbitals, do not contribute in calculations of rotatory strengths.

The dipole transition strength in RPA is size intensive [25]. Due to the guage-origin dependence the length formula for rotatory strength in conventional basis sets is not size intensive in RPA. On the contrary, since both the velocity formula and the LAO-length formula for rotatory strength are gauge-origin independent, RPA calculations of rotatory strength are size intensive when these two formulas are used.

3. Calculation

The LAO formulas for rotatory strength in electronic circular dichroism in the length form have been implemented in the ABACUS [26] program for SCF and MCSCF wave functions. The SCF implementation gives RPA response functions [16, 17] and the MCSCF implementation gives MC-RPA response functions [24]. The rotatory strength are the residues of these response functions. In the LAO implementation the conventional magnetic dipole operator is replace by the corresponding LAO operator (36). The RPA calculations are carried out in the atomic orbital basis with no reference to molecular orbital integrals. Our implementation also includes the conventional basis length and velocity formulas for rotatory and oscillator strengths [1].

We have investigated with the SIRIUS/ABACUS [26, 27] program package the optically active molecule *trans*-cyclooctene (TCO). Experimentally, both absorption and CD spectra have been recorded [20]. TCO is a prototype of inherently dissymmetric molecules and has been the subject of many theoretical investigations. Some of the first were semiempirical [21] and minimal basis *ab initio* calculations [28]. The CD spectrum has also been modelled in CI calculations on the TCO ethylene fragment, i.e., ethylene where the geometry is fixed as in the double bonded carbon structure of TCO [29]. The CD spectra of TCO and its ethylene and butylene fragments have been calculated in the RPA approximation by Hansen and Bouman, who used localized orbitals to characterize the individual transitions and to decompose the rotatory strength into distinct contributions [22]. The simulated spectra of TCO were in fair agreement with experiments, while little regularity was observed in the spectra for TCO and its ethylene and butylene fragments.

In this work the CD and absorption spectra of TCO and its ethylene (TCO-E), butylene (TCO-B), and hexene (TCO-H) fragments have been determined at the LAO RPA level. The calculations on TCO-E were used to select a basis for the larger systems and to compare the LAO rotatory strengths with non-London velocity and length calculations. The calculations here presented are closer to the RPA basis set limit than previous results and can therefore be used more reliably to compare the spectra of TCO and its fragments.

The calculations were performed partly on a Convex 3840 and partly on a Cray 92A. The computationally most demanding calculation was the one on TCO with 216 basis functions (see below) and it took 4 h and 40 min of cpu time on the Cray 92A.

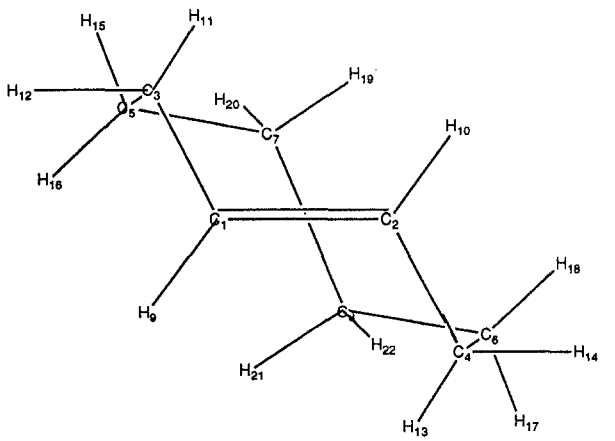

Fig. 1. The structure of (−)-*trans*-cyclooctene (TCO) with labelling of atoms

A. Geometries and basis sets

We have used the geometries of Hansen and Bouman in the calculations on TCO (Fig. 1), TCO-E, and TCO-B [22, 30]. The geometry of TCO-H is in analogy with TCO-E and TCO-B obtained by replacing the C_5–C_7 and C_6–C_8 bonds in TCO by C–H bonds of 1.12 Å (see Fig. 1). The guage origin is in all calculations at the center of the C_1–C_2 double bond.

We have used six basis sets in our calculations on TCO-E. In order of increasing size these basis sets are denoted A, B, C, D, E, and F. The A basis is the one used by Hansen and Bouman in calculations on TCO-E [22]. It is a double zeta basis augmented with split diffuse *s* and *p* functions on carbon. The remaining sets are generated from Dunning's augmented correlation consistent pVDZ and pVTZ basis sets [31–33]. For basis B we used the aug-cc-pVDZ basis, but omitted the *p* functions on hydrogen and the most diffuse *d* function on carbon. Extra diffuse *s* ($\alpha = 0.015633$) and *p* ($\alpha = 0.013470$) functions were added on carbon. The C basis is obtained from B by adding a diffuse *s* ($\alpha = 0.009913$) function on hydrogen. Basis D is identical to C except that the hydrogen *p* function of the cc-pVDZ basis is included. The E basis consists of the aug-cc-pVDZ basis augmented with the same diffuse functions that were added to obtain the B and C sets. The largest basis, F, corresponds to the aug-cc-*p*VTZ basis minus the two *f* functions on carbon, plus extra diffuse functions *s* ($\alpha = 0.014673$) and *p*($\alpha = 0.011897$) on carbon and *s* ($\alpha = 0.008420$) on hydrogen.

B. Results for TCO-E

The parent molecule TCO and the fragment molecules have C_2 symmetry and an *A* ground state. We have carried out RPA [16, 17] calculations to the eight lowest states of both *A* and *B* symmetry for TCO-E. The Hartree–Fock ground state total energies are listed in Table 1, and the excitation energies are plotted as function of basis sets in Fig. 2a and b. The four lowest excitation energies of *A* symmetry are relatively stable towards basis set extensions. The next three *A*-excitation energies

Table 1. Energies (in Hartree) obtained for the indicated molecules and basis sets

Molecule	Basis	Size[a]	Energy
TCO-E	A	42	− 77.998 291
TCO-E	B	56	− 78.015 685
TCO-E	C	60	− 78.015 746
TCO-E	D	72	− 78.028 801
TCO-E	E	94	− 78.030 285
TCO-E	F	128	− 78.048 088
TCO-B	C	120	− 156.079 418
TCO-H	C	180	− 234.132 092
TCO	C	216[b]	− 311.031 901

[a] Size is the number of basis functions

[b] There are 232 AO basis functions but due to linear dependencies are six OMOs of *A* symmetry and ten OMOs of *B* symmetry left out of the calculation

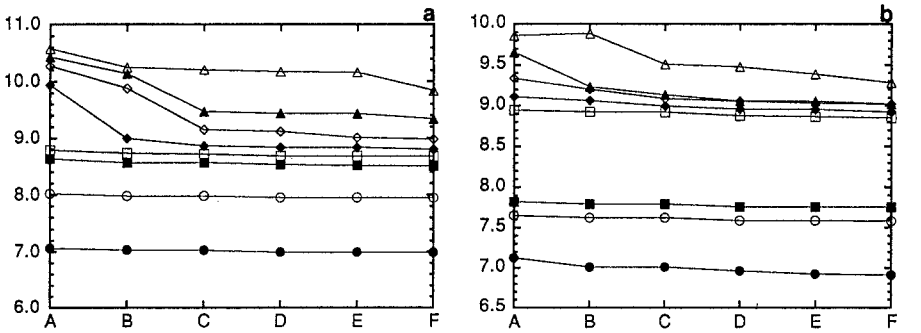

Fig. 2a. Plot of calculated excitation energies (eV) for transitions from the ground electronic state of TCO-E to the eight lowest lying excited states of *A* symmetry as function of basis set. **b** Plot of calculated excitation energies (eV) for transitions from the ground electronic state of TCO-E to the eight lowest lying excited states of *B* symmetry as function of basis set

are relatively stable after the C basis. For excitations of *B* symmetry the five first transitions are fairly stable for all basis sets, while the three remaining transitions are relatively stable from basis C. These observations suggest that basis C is adequate for the calculations on the other fragments and TCO.

The rotatory strengths calculated from the velocity, length, and LAO formulas are in the Fig. 3a–d plotted as functions of the basis set for the lowest two excitations of each symmetry. It is reassuring to note that the three formulas converge to the same values for basis F for all four rotatory strengths. The LAO formula gives better basis set convergence for three of the four rotatory strengths (1*A*, 1*B*, and 2*B*). This happens since the LAOs respond in a physically reasonable way to the external magnetic field. The rotatory strengths are dot products of the magnetic and electric dipole transition moments. The LAO basis does not improve on the descriptions of the electric dipole moments and the excited states. Therefore, the basis set convergence does not improve as spectacularly as in calculations of

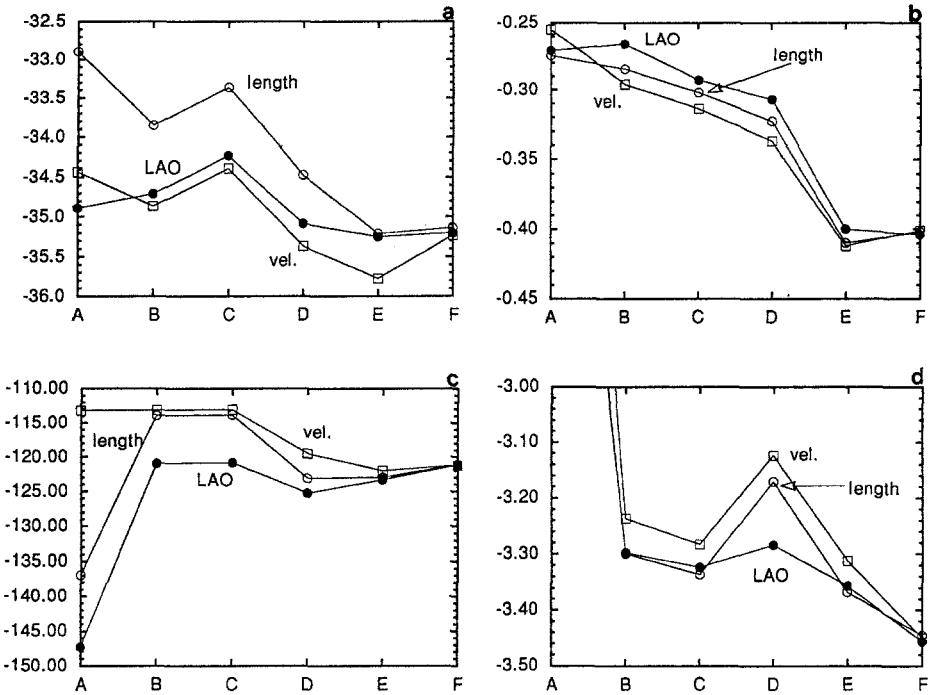

Fig. 3a. Plot of rotatory strengths (10^{-40} esu) calculated from the LAO, the velocity, and the length formula, as function of basis set for the first transition from the ground state of TCO-E to an *A* state. **b** Plot of rotatory strengths (10^{-40} esu) calculated from the LAO, the velocity, and the length formula, as function of basis set for the second transition from the ground state of TCO-E to an *A* state. **c** Plot of rotatory strengths (10^{-40} esu) calculated from the LAO, the velocity, and the length formula, as function of basis set for the first transition from the ground state of TCO-E to a *B* state. **d** Plot of rotatory strengths (10^{-40} esu) calculated from the LAO, the velocity, and the length formula, as function of basis set for the first transition from the ground state of TCO-E to a *B* state

magnetizabilities and atomic axial tensors. The results in Fig. 3 further support our conclusion that basis C should be used for the calculations on the other fragments and TCO.

C. Comparing the results of TCO-E, TCO-B, TCO-H, and TCO

For the calculations on TCO-B, TCO-H, and TCO we have used basis C as suggested by the TCO-E results. For TCO this amounts to 232 AO basis functions.

Ground state energies are listed in Table 1, and the frequencies, oscillator strengths, and rotatory strengths calculated for the eight lowest excitations of each symmetry are listed in Table 2. In Fig. 4a and b the frequencies are plotted as functions of basis set. These figures show that the excitation energies change significantly when going from TCO-E to TCO-B but only slightly going from TCO-B over TCO-H to TCO. As seen from Table 2, the oscillator and rotatory strengths change significantly from one molecule to another. Compared to TCO,

Table 2. Frequencies in eV, oscilator strength, and rotational strengths (10^{-40} esu) as calculated from basis C for TCO-E, TCO-B, TCO-H, and TCO for the for the eight first transitions of each symmetry

	Frequencies				Oscilator strength (length)				Rotational strength (LAO)			
Transition	TCO-E	TCO-B	TCO-H	TCO	TCO-E	TCO-B	TCO-H	TCO	TCO-E	TCO-B	TCO-H	TCO
1*A*	7.03	6.37	6.53	6.60	0.075	0.006	0.029	0.028	− 34.24	− 4.92	− 5.01	− 4.44
2A	7.98	6.98	7.07	7.29	0.004	0.024	0.000	0.002	− 0.29	2.68	− 0.09	1.75
3*A*	8.57	7.62	7.59	7.62	0.009	0.004	0.006	0.004	− 9.90	1.54	8.82	6.37
4*A*	8.72	7.67	7.64	7.67	0.000	0.009	0.000	0.000	− 0.06	− 4.62	− 1.00	− 2.47
5*A*	8.86	7.76	7.69	7.76	0.006	0.001	0.019	0.022	− 3.01	1.64	− 2.93	− 2.33
6*A*	9.15	7.97	7.91	7.96	0.071	0.000	0.008	0.006	28.99	0.34	− 1.23	− 1.06
7*A*	9.47	8.15	8.13	8.28	0.001	0.007	0.000	0.009	0.99	1.56	0.16	4.76
8*A*	10.20	8.48	8.25	8.33	0.006	0.001	0.001	0.001	− 1.94	− 0.28	0.06	− 0.17
1*B*	7.01	6.55	6.52	6.53	0.331	0.230	0.183	0.101	− 120.83	− 36.69	− 38.45	− 25.73
2B	7.62	6.78	6.80	6.94	0.004	0.031	0.167	0.214	− 3.32	− 14.68	− 12.86	− 75.44
3*B*	7.79	7.12	7.12	7.17	0.010	0.023	0.026	0.004	0.89	− 40.60	− 6.34	16.19
4*B*	8.92	7.74	7.65	7.71	0.000	0.025	0.024	0.015	− 1.37	7.55	− 4.67	− 4.73
5*B*	8.99	7.84	7.79	7.79	0.001	0.048	0.008	0.005	7.25	16.68	− 7.70	− 9.69
6*B*	9.08	8.01	7.89	7.93	0.004	0.001	0.000	0.001	2.09	− 0.70	0.41	− 2.37
7*B*	9.13	8.15	8.06	8.14	0.059	0.007	0.004	0.000	145.78	− 14.89	− 5.09	− 0.30
8*B*	9.51	8.34	8.22	8.31	0.032	0.005	0.011	0.008	5.59	− 1.86	4.67	8.00

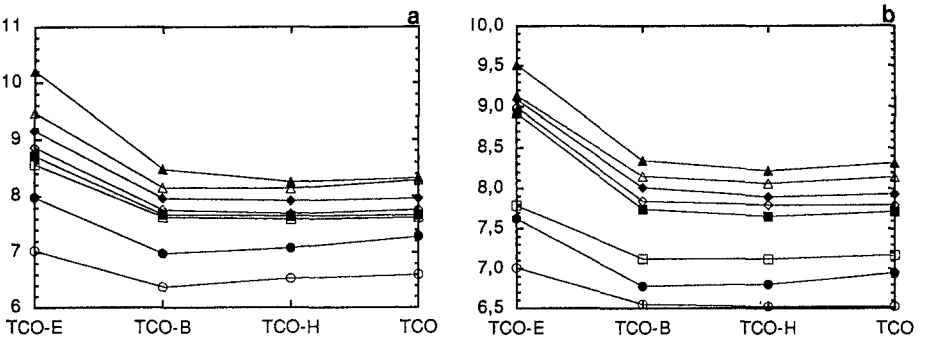

Fig. 4a. Plot of calculated excitation energies (eV) for the transitions to the eight lowest lying excited *A* states as function of molecule. The C basis has been used in these calculations. **b** Plot of calculated excitation energies (eV) for the transitions to the eight lowest lying excited *B* states as function of molecule. The C basis has been used in these calculations

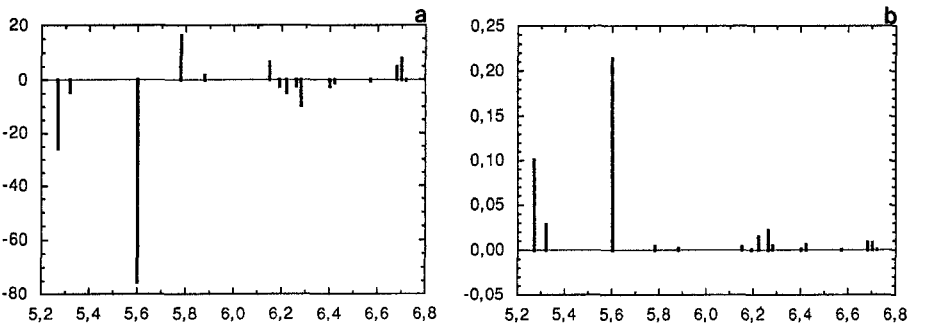

Fig. 5a. The 16 calculated rotatory strengths (10^{-40} esu) of (−)-*trans*-cyclooctene plotted as a CD spectrum. **b** The 16 calculated oscillator strengths of (−)-*trans*-cyclooctene plotted as an absorption spectrum

we see that for TCO-H only 4 out of the 16 oscillator strengths and 8 out of the 16 rotatory strengths are less than 50% off. Correspondingly, for TCO-B 5 oscillator strengths and 2 rotatory strengths are less than 50% off, and for TCO-E the numbers are 0 and 1.

Our calculations demonstrate quite clearly that the absorption and CD spectra of TCO cannot be generated from any of the fragment molecules, although the number of strengths that agree increases with the size of the fragment. This observation agrees with the finding of Hansen and Bouman, although their frequencies, oscillator, and rotatory strengths differ from the values obtained here [22]. For TCO-E in basis A, the differences between the previous [22] and the present results are minor and are believed to stem from differences in implementation and convergence criteria. For TCO the previous calculation [22] used a basis smaller than A for non-chromophoric atoms.

To aid the comparison of the calculated TCO numbers with the experimental spectra of Mason and Schnepp [20], we have in Fig. 5a, b plotted the calculated absorption and CD spectra without simulating the line shapes of the individual partial and differential absorptions. Note that the experimental spectrum is for

(+)-TCO while our calculations are for (−)-TCO. Therefore, the calculated and experimental rotatory strengths have opposite signs.

The first significant feature in both experimental spectra are bands around $5.1 \times 10^4\ cm^{-1}$, corresponding to a transition that has been characterized as $\pi \rightarrow \pi^*$ in the ethylene chromophore [20]. The sum of the rotatory strengths of this transition and the two weaker transitions at 4.7×10^4 and $5.6 \times 10^4\ cm^{-1}$ is experimentally determined as 92×10^{-40} esu [20]. The contributions from the weaker transitions have the same signs as the strong transition and are estimated to be 20% and 10%, respectively, of the total rotatory strength [20].

The calculated absorption and rotatory strengths at $5.6 \times 10^4\ cm^{-1}$ correspond to the experimental transition at $5.1 \times 10^4\ cm^{-1}$. Two transitions are calculated around $5.3 \times 10^4\ cm^{-1}$. The rotatory strengths of these transitions have the same signs as the stronger rotatory strength at $5.6 \times 10^4\ cm^{-1}$. These transitions are taken to correspond to the experimental transition at $4.7 \times 10^4\ cm^{-1}$. Two transitions are also calculated around $5.8 \times 10^4\ cm^{-1}$. Although the rotatory strengths of these transitions have opposite signs of the strong rotatory strength at $5.6 \times 10^4\ cm^{-1}$, these transitions are taken to correspond to the experimental transition observed at $5.6 \times 10^4\ cm^{-1}$. The sum of these five calculated rotatory strengths is -88×10^{-40} esu, which corresponds nicely to the experimental value above. The contribution to this value from the two transitions around $5.3 \times 10^4\ cm^{-1}$ amounts to 35%. Correspondingly, the contributions from the transitions around $5.8 \times 10^4\ cm^{-1}$ amount to −21%. The calculated numbers are thus in reasonable agreement with experiment, although they indicate that the experimental bands at 4.7×10^4 and $5.6 \times 10^4\ cm^{-1}$ are both a sum of two transitions, and that the band calculated around $5.8 \times 10^4\ cm^{-1}$ has the sign reversed to what is inferred from the experiment.

The second significant band in the experimental CD spectrum [20] has the opposite sign of the first one and peaks around $6.4 \times 10^4\ cm^{-1}$. Assuming a similar displacement of this peak as for the first peak, we expect that this transition should appear around $6.9 \times 10^4\ cm^{-1}$. However, all 16 excitations we have calculated have frequencies smaller than $6.72 \times 10^4\ cm^{-1}$ and this peak is therefore not observed in our calculations.

4. Concluding remarks

We have derived the second-quantization magnetic dipole operator that arises when London atomic orbitals are used. This operator depends on the LAOs, but in the final expression for the operator the integrals involve conventional AOs only. The resulting magnetic dipole operator is a two-electron operator, which converges to the exact operator in the limit of a complete basis set. For finite basis sets, the operator depends on the gauge origin in exactly the same manner as the exact operator. Rotatory strengths calculated in the length expression from this operator are origin independent in finite basis linear response calculations such as RPA and MC-RPA.

The presented calculations on *trans*-cyclootene and its fragments, indicate that the basis set convergence of rotatory strength is favorable for calculations using the derived operator in the length formula as compared to conventional calculations based on standard basis sets. The calculated absorption and CD spectra are closer to the RPA limit than previous calculations, and the calculated spectra compare well with experiment. As concluded by Hansen and Bouman [22] little regularity is

found when comparing the spectra of TCO and its fragments. Therefore, little information about the TCO spectra can be deduced from calculations on the fragments.

Acknowledgements. This work has been partly supported by the Danish Natural Science Research Council (Grant No. 11-0924 and 5210506-3) and Nordisk Forskeruddannelsesakademi.

References

1. Hansen AaE, Bouman TD (1980) Adv Chem Phys 44:545
2. London F (1937) J Phys Radium 8:397
3. Hameka HF (1958) Mol Phys 1:203
4. Hameka HF (1959) Z Naturforsch 14a:599
5. Mc Weeny R (1958) Mol Phys 1:311
6. Seamans L, Linderberg J (1972) Mol Phys 24:1393
7. Dalgaard E (1978) Proc R Soc Lond A 361:487
8. Ditchfield R (1972) J Chem Phys 56:5688
9. Wolinski K, Hinton JF, Pulay P (1990) J Am Chem Soc 112:8251
10. Gauss J (1992) Chem Phys Lett 191:614
11. Ruud K, Helgaker T, Kobayashi R, Jørgensen P, Bak KL, Jensen HJAa (1994) J Chem Phys 100:8178
12. Ruud K, Helgaker T, Bak KL, Jørgensen P, Jensen HJAa (1993) J Chem Phys 99:3847
13. Ruud K, Skaane H, Helgaker T, Bak KL, Jørgensen P (1994) J Am Chem Soc
14. Bak KL, Jørgensen P, Helgaker T, Ruud K Jensen HJAa (1993) J Chem Phys 98:8873
15. Bak KL, Jørgensen P, Helgaker T, Ruud K Jensen HJAa (1994) J Chem Phys 100:6620
16. McLachlan AD, Ball MA (1964) Rev Mod Phys 36:844
17. Linderberg J, Öhrn Y (1973) Propagators in quantum chemistry. Academic Press, New York
18. Olsen J, Jørgensen P (1985) J Chem Phys 82:3235
19. Olsen J, Bak KL, Helgaker T, Ruud K, Jørgensen P, Theoret Chem Acta submitted
20. Mason MG, Schnepp O (1973) J Chem Phys 59:1092
21. Levi CC, Hoffmann R (1972) J Am Chem Soc 94:3446
22. Hansen AaE, Bouman TD (1985) J Am Chem Soc 107:4828
23. Helgaker T, Jørgensen P (1991) J Chem Phys 95:2595
24. Yeager DL, Jørgensen P (1979) Chem Phys Lett 65:77
25. Koch H, Helgaker T, Jørgensen P (1990) J Chem Phys 93:3345
26. Helgaker T, Bak KL, Jensen HJAa, Jørgensen P, Kobayashi R, Koch H, Mikkelsen K, Olsen J, Ruud K, Taylor PR, Vahtras O, ABACUS, a second-order MCSCF molecular property program
27. Jensen HJAa, Ågren H, SIRIUS, a program for calculation for MCSCF wave functions
28. Rauk A, Barriel JM, Ziegler T (1977) Prog Theoret Org Chem 2:467
29. Liskow DH, Segal GA (1978) J Am Chem Soc 100:2945
30. The dihedral angle H–C_1–C_2–H in Ref [22], Table 1 is misprinted as 188.9. The correct value is −188.9
31. Dunning THJr (1989) J Chem Phys 90:1007
32. Kendall RA, Dunning THJr, Harrison RJ (1992) J Chem Phys 96:6796
33. Woon DE, Dunning THJr (1993) J Chem Phys 98:1358